Available online at www.sciencedirect.com
ScienceDirect
Ceramics International 34 (2008) 263–268
CERAMICS INTERNATIONAL
www.elsevier.com/locate/ceramint

Large-scale fine structural alumina matrix ceramic guideway materials improved by diopside and Fe_2O_3

Changxia Liu [a,b,*], Jianhua Zhang [a,*], Xihua Zhang [c], Junlong Sun [a,b]

[a] Department of Mechanical Engineering, Shandong University, Jinan 250061, Shandong Province, PR China
[b] Communications Institute, Ludong University, Yantai 264025, Shandong Province, PR China
[c] Department of Materials Science and Engineering, Shandong University, Jinan 250061, Shandong Province, PR China

Received 3 July 2006; received in revised form 25 July 2006; accepted 2 September 2006
Available online 7 November 2006

Abstract

Diopside and Fe_2O_3 were introduced in alumina matrix ceramic materials. Large-scale fine structural alumina matrix ceramic guideway materials were fabricated by the technology of pressureless sintering, during which liquid phase sintering took place and new phases such as $3Al_2O_3{\cdot}2SiO_2$, $CaO{\cdot}Al_2O_3{\cdot}2SiO_2$ and $CaO{\cdot}6Al_2O_3$ were produced by the chemical reactions taking place among alumina and the additives. The hardness, the fracture toughness and the bending strength of the guideway products were tested. The influences of diopside and Fe_2O_3 additions were studied by microstructural observations and mechanical properties evaluations. Meanwhile, the expected improvement of mechanical properties compared with pure alumina was indeed observed. The fracture mechanism and porosity of large-scale fine structural alumina matrix ceramic guideway materials were analyzed.

Keywords: Alumina; Diopside; Fe_2O_3; Guideway; Large-scale fine structural ceramics

1. Introduction

Alumina matrix ceramic materials are widely applied in the fields of mechanical engineering [1–4], electronic technology [5], chemical engineering [6–9] and biological engineering [10]. Machine tool guideway in mechanical engineering demands for excellent wear resistance and low friction coefficient, conventional guideway materials such as cast iron (quenched include), steel, plastics, and polymeric compounds always have a short length of life. These materials may be likely to give way to fine alumina matrix ceramic materials for their virtues of high hardness, good chemical inertness, high wear resistance, low coefficient of thermal expansion and low friction coefficient. However, the brittleness of pure alumina limits its potential applications, and excellent mechanical properties are obtained always companied with a cost increase on account of the expensive second phases [11–15]. It generally costs more when fabricating ceramic guideway materials owing to its large dimension. So low-cost also may be regarded as a priority when researchers design the compositions of large-scale fine alumina matrix ceramic guideway materials. Diopside ($MgCa(SiO_3)_2$) and Fe_2O_3 just has the virtue of low-cost by contrast to other additives. The sources of α-Al_2O_3, diopside and Fe_2O_3 are in abundance in China and their price is low. Fe_2O_3 is generally used as a nucleant agent of glass-ceramics [16,17]. Diopside acts as an accessory ingredient in the sintering process and decreases the sintering temperature of alumina matrix ceramic materials. As for large-scale fine structural alumina matrix ceramic guideway products, their large dimension and complicated shape make it difficult to fabricate these ceramic materials by the process of hot-pressing. So pressureless sintering technology was chosen and liquid phase sintering can take place during the process of sintering.

In this paper, large-scale fine structural alumina matrix ceramic guideway materials with different contents of diopside and Fe_2O_3 were fabricated by pressureless sintering technology in a furnace without any atmosphere protection. The specific objective of the study is to investigate the effects of diopside

* Corresponding authors.
E-mail addresses: hester5371@gmail.com (C. Liu), jhzhang@sdu.edu.cn (J. Zhang).

0272-8842/$34.00
doi:10.1016/j.ceramint.2006.09.014

and Fe_2O_3 on mechanical properties, degree of porosity and microstructures of large-scale fine structural alumina matrix ceramic guideway materials.

2. Experimental procedure

Commercial Al_2O_3 powder of high purity (99.99%) and small grain size (0.5–1 μm) was used as the starting materials. Fe_2O_3 and diopside ($MgCa(SiO_3)_2$), which is composed of SiO_2 (55 wt.%), CaO (24 wt.%) and MgO (18 wt.%), were used as additives. The content of diopside and Fe_2O_3 is listed in Table 1 (the suffixes in AD_0F_0, AD_5F_0, AD_5F_3, $AD_{10}F_0$ and $AD_{10}F_3$ represent the weight content of diopside and Fe_2O_3. For example, $AD_{10}F_3$ means the content of diopside and Fe_2O_3 are 10 and 3 wt.%, respectively).

First, the raw materials were blended with each other according to certain proportions and ball milled for 60 h in an alcohol medium to obtain an homogeneous mixture. Second, the slurry was dried in vacuum and screened. Third, the green bodies of guideway (1800 mm × 150 mm × 50 mm) were shaped by slip casting process and then dense green bodies of guideway are obtained by using isostatic cool pressing technology in rubber molds. Lastly, pressureless sintering was used to sinter these dense green bodies in a furnace in air. The green bodies of guideway were heated up to 1500 °C according to a temperature gradient [18], as listed in Table 2.

The sintered guideway products were cut into specimens by an inside diameter slicer. Standard test pieces (3 mm × 4 mm × 36 mm) were obtained through rough grinding, finish grinding with diamond wheels and polishing. Three-point bending mode was used to measure the bending strength on an electronic universal experimental instrument (WD-10) with a span of 20 mm at a crosshead speed of 0.5 mm/min. Twelve specimens, chosen from one guideway product with the same compositions, were used for measuring the bending strength in air at room temperature. The bending strength was calculated by the following formula [19]:

$$\sigma_f = \frac{3PL}{2bh^2} \quad (1)$$

where σ_f is the bending strength (MPa), P is the load (N) under which the samples break, b and h are width and height (mm), respectively, and L is the span (mm).

Vickers hardness was measured on polished surface with a load of 9.8 N for 5 s with a micro-hardness tester (MH-6). Fracture toughness measurement was performed using indentation method with a hardness tester (Hv-120), and results were obtained by the formula proposed by Cook and Lawn [20].

Table 1
Compositions of alumina matrix ceramic guideway materials

Specimens	Compositions (wt.%)
AD_0F_0	100% Al_2O_3
AD_5F_0	5% diopside + 95% Al_2O_3
AD_5F_3	5% diopside + 92% Al_2O_3 + 3% Fe_2O_3
$AD_{10}F_0$	10% diopside + 90% Al_2O_3
$AD_{10}F_3$	10% diopside + 87% Al_2O_3 + 3% Fe_2O_3

Table 2
Temperature gradient of pressureless sintering process (115 h) [18]

Temperature (°C)	Speed of heating up and cooling (°C/h)
20–300	10
300–600	20
600–900	30
900–1500	40
1500	3 h holding
1500–1000	20
1000–50	50
50	Open the furnace door

XRD (D/max-2400) analysis was undertaken to identify the crystal phases after sintering. The microstructures of the specimens were studied on fracture surfaces and polished surfaces by scanning electron microscopy (HITACHI S-570).

3. Results and discussion

3.1. X-ray diffraction phase analysis

The X-ray diffraction phase analysis of AD_5F_0 and AD_5F_3 specimens are shown in Figs. 1 and 2, respectively. It is clear from Figs. 1 and 2 that there exist in AD_5F_0 and AD_5F_3 the newly formed $3Al_2O_3{\cdot}2SiO_2$, $CaO{\cdot}Al_2O_3{\cdot}2SiO_2$ and $CaO{\cdot}6Al_2O_3$ phases. Theoretically there should exist $MgO{\cdot}Al_2O_3$ in the composites, but XRD analysis did not show the occurrence of

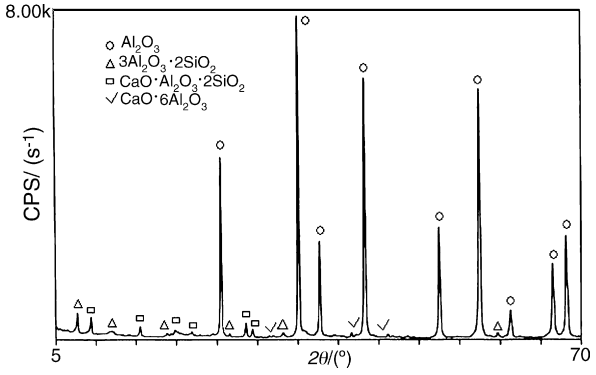

Fig. 1. X-ray diffraction phase analysis of AD_5F_0 specimen.

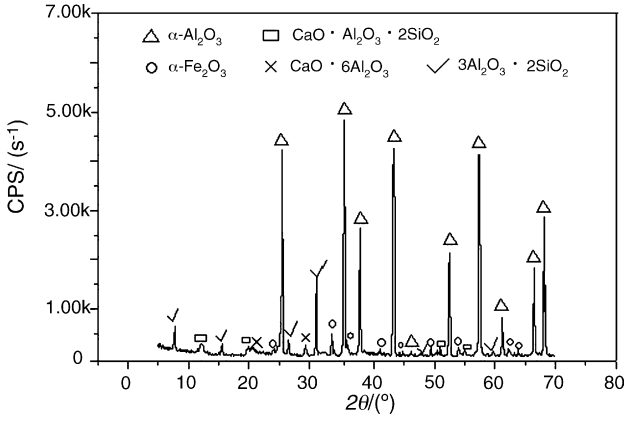

Fig. 2. X-ray diffraction phase analysis of AD_5F_3 specimen.

Table 3
Mechanical properties of alumina matrix ceramic guideway materials

Specimens	Bending strength (MPa)	Fracture toughness (MPa $m^{1/2}$)	Hardness (GPa)	Relative density (%)
AD_0F_0	113.0	3.27	5.6	90.2
AD_5F_0	320.6	4.62	12.0	92.7
AD_5F_3	335.5	4.51	12.8	92.9
$AD_{10}F_0$	341.0	4.10	13.5	94.0
$AD_{10}F_3$	349.3	4.32	14.4	94.3

$MgO{\cdot}Al_2O_3$. This is because the content of diopside is only 5 wt.% in the composites, and that of MgO is 18 wt.% in diopside, so the percent of MgO in the composites is only 0.9 wt.% and thus the amount of $MgO{\cdot}Al_2O_3$, produced by the reaction taking place between MgO and Al_2O_3, is too small to be detected by XRD analysis.

The sintering temperature (1500 °C) is higher than the melting point of diopside (1300–1390 °C). Hence liquid phase sintering takes place and the following chemical reactions, yielding mullite, anorthite and $CaO{\cdot}6Al_2O_3$, may occur during the sintering process:

$$3Al_2O_3 + 2SiO_2 \rightarrow 3Al_2O_3{\cdot}2SiO_2 \quad (2)$$

$$CaO + Al_2O_3 + 2SiO_2 \rightarrow CaO \cdot Al_2O_3{\cdot}2SiO_2 \quad (3)$$

$$6Al_2O_3 + CaO \rightarrow CaO \cdot 6Al_2O_3 \quad (4)$$

Based on thermodynamic analysis of the reactions, we can get the following rankings [21]:

$$\Delta G^{\theta}_{T2} < 0, \quad \Delta G^{\theta}_{T3} < 0, \quad \Delta G^{\theta}_{T4} < 0$$

where $\Delta G^{\theta}_{T2}, \Delta G^{\theta}_{T3}$ and ΔG^{θ}_{T4} represent the Gibbs free energy of the Eqs. (2)–(4), respectively. XRD analysis shows that mullite, anorthite and $CaO{\cdot}6Al_2O_3$ actually exist in specimen of AD_5F_0 and AD_5F_3 as previously mentioned. The existing of mullite in large-scale fine structural alumina matrix ceramic guideway materials may be helpful to make the composite has a high potential for wear resistance applications [1].

3.2. Mechanical properties

Mechanical properties of pressureless sintered large-scale fine structural alumina matrix ceramic guideway materials are listed in Table 3. As seen from Table 3, the bending strength, fracture toughness and hardness of pressureless sintered pure alumina are 113.0 MPa, 3.27 MPa $m^{1/2}$ and 5.6 GPa, respectively. Addition of diopside and Fe_2O_3 significantly improves the performances of pressureless sintered guideway composites. The bending strength and hardness of guideway composites increase with increasing the amount of diopside, and addition of Fe_2O_3 promotes this trend of improvement when the content of diopside is identical, then reach their maximum value of 349.3 MPa and14.4 MPa $m^{1/2}$, respectively. This is because diopside and Fe_2O_3 all improve the densification rate of the composites (relative density in Table 3). Kim et al. [22] has observed that the mechanical properties of the composites increased with the increasing of the relative density of sintered specimens. So addition of diopside and Fe_2O_3 may be helpful to improve the mechanical properties of large-scale fine structural alumina matrix ceramic guideway materials. The variation of fracture toughness of guideway composites changing with content of diopside and Fe_2O_3 is a little indistinct, it reaches its maximum value of 4.62 MPa $m^{1/2}$ in AD_5F_0 specimen. The mechanical properties of guideway composites are also to a great extent relevant to their microstructures, which will be discussed in the following section.

It is obvious that the fabricated large-scale fine structural alumina matrix ceramic guideway materials, pressureless sintered at 1500 °C for 3 h in air, exhibit significant improvements in mechanical properties compared to pure Al_2O_3. Composite with the addition of 10 wt.% diopside and 3 wt.% Fe_2O_3 ($AD_{10}F_3$ specimen) shows better comprehensive performances, the bending strength, fracture toughness and the hardness of the composite reach 349.3 MPa, 4.32 MPa $m^{1/2}$ and 14.4 GPa, respectively, which are enhanced by 209.1%, 32.1% and 157.1%, respectively, with respect to pure Al_2O_3 pressureless sintered under the same conditions.

3.3. Analysis of microstructures

SEM photomicrograph on fracture surface of pure alumina pressureless sintered at 1500 °C is shown in Fig. 3, those of AD_5F_0, $AD_{10}F_0$ and $AD_{10}F_3$ are shown in Figs. 4–6,

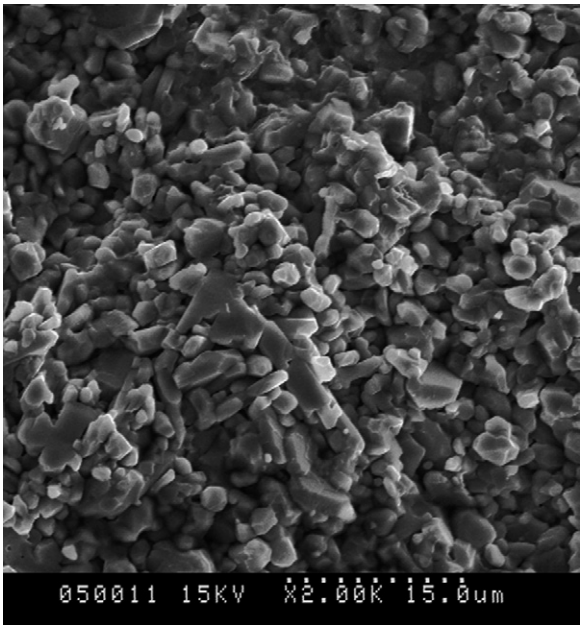

Fig. 3. SEM photomicrograph on fracture surface of pure Al_2O_3.

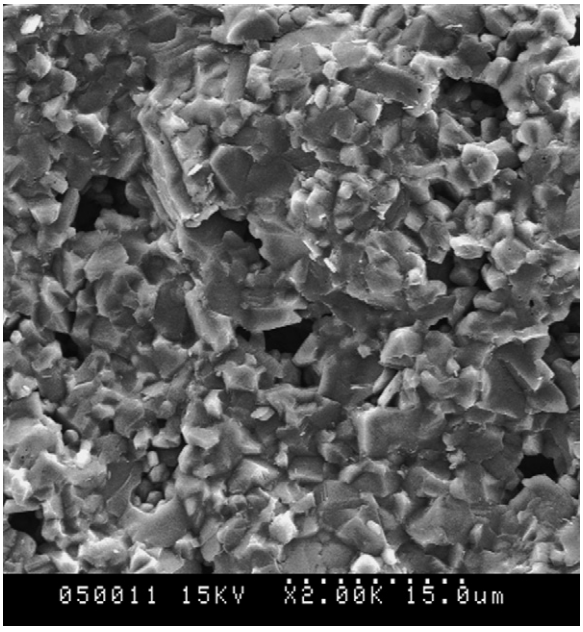

Fig. 4. SEM photomicrograph on fracture surface of AD_5F_0 specimen.

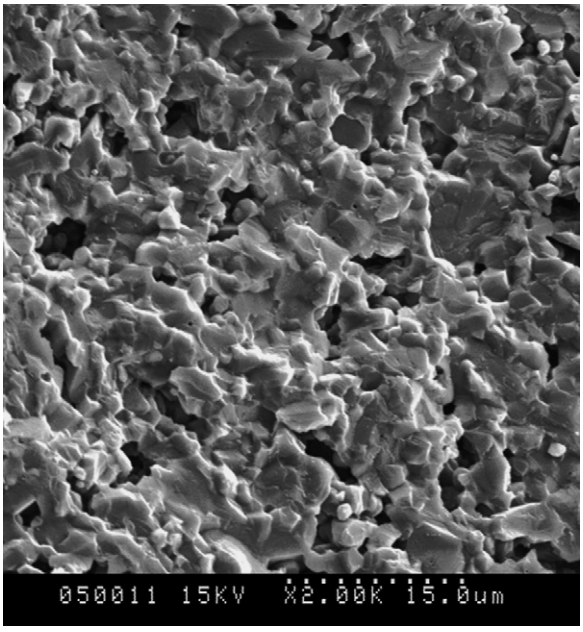

Fig. 6. SEM photomicrograph on fracture surface of $AD_{10}F_3$ specimen.

respectively. As seen from Fig. 3, the grain shapes of pure alumina are irregular and there appears abnormal growth. While in Figs. 4–6, the guideway composites, sintered under the same conditions, show a homogeneous distribution of alumina grains and additive particles. The microstructures of alumina matrix ceramic guideway composites are finer than that of pure alumina.

The fracture mode of pure alumina is mainly intergranular failure. While that of AD_5F_0, $AD_{10}F_0$ and $AD_{10}F_3$ show a combination of intergranular failure and transgranular failure. Further addition of diopside makes the occurrence of transgranular failure more than that of intergranular failure (Figs. 4 and 5). The microstructure of $AD_{10}F_3$ is analogous to that of $AD_{10}F_0$ except that $AD_{10}F_3$ specimen shows a little more homogeneous and finer microstructure than $AD_{10}F_0$ (Figs. 5 and 6). Obviously, when the amount of diopside is identical, addition of Fe_2O_3 makes the microstructure of guideway composites a little more homogeneous and finer, which may bring on the improvements in bending strength of large-scale fine structural alumina matrix ceramic guideway materials.

As seen from the microstructures of pure alumina, AD_5F_0, $AD_{10}F_0$ and $AD_{10}F_3$, the bondings of grains become stronger when the fracture mode turns to the combination of transgranular failure and intergranular failure. In other words,

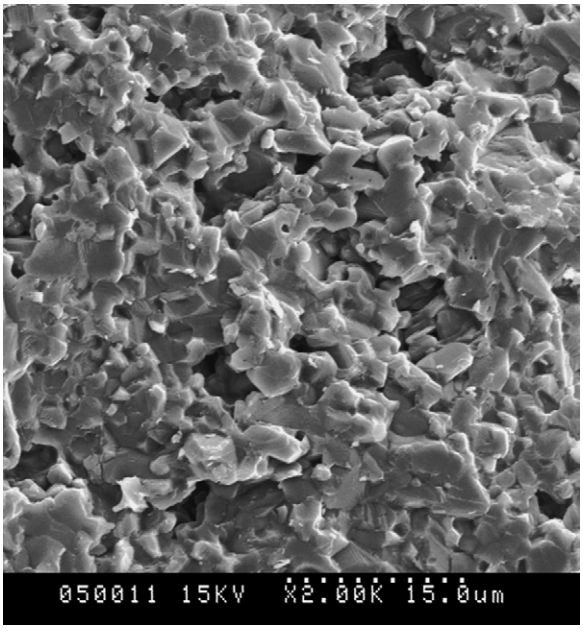

Fig. 5. SEM photomicrograph on fracture surface of $AD_{10}F_0$ specimen.

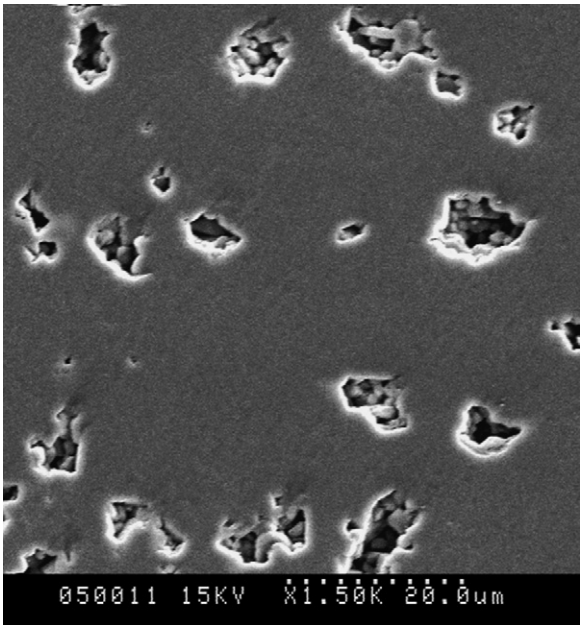

Fig. 7. SEM photomicrograph on polished surface of AD_5F_0 specimen.

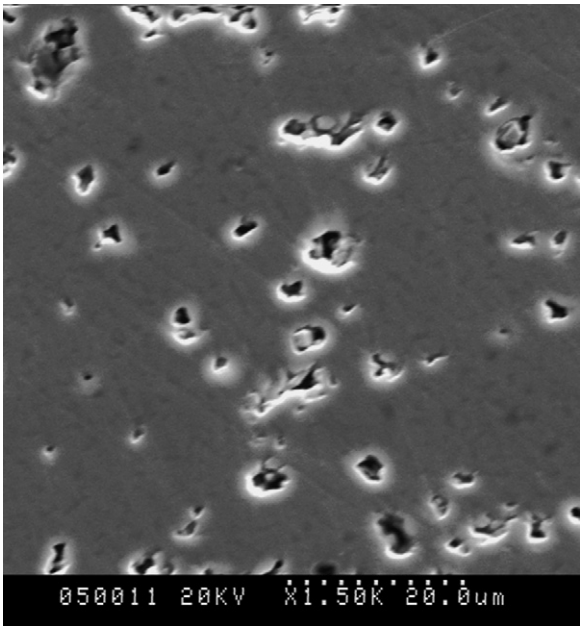

Fig. 8. SEM photomicrograph on polished surface of AD_5F_3 specimen.

a fracture mode changing from intergranular failure to the combination of transgranular failure and intergranular failure is observed and may bring on a significant increase in bending strength and fracture toughness. The main cause is that the grain boundaries of large-scale fine structural alumina matrix ceramic guideway materials are strengthened owing to the addition of diopside and Fe_2O_3.

Figs. 7–9 respectively show the SEM photomicrographs on polished surfaces of AD_5F_0, AD_5F_3 and $AD_{10}F_0$ specimens. As seen from these figures, there exist apparent pores on the polished surface of large-scale fine structural alumina matrix ceramic guideway materials, which may be difficult to avoid in

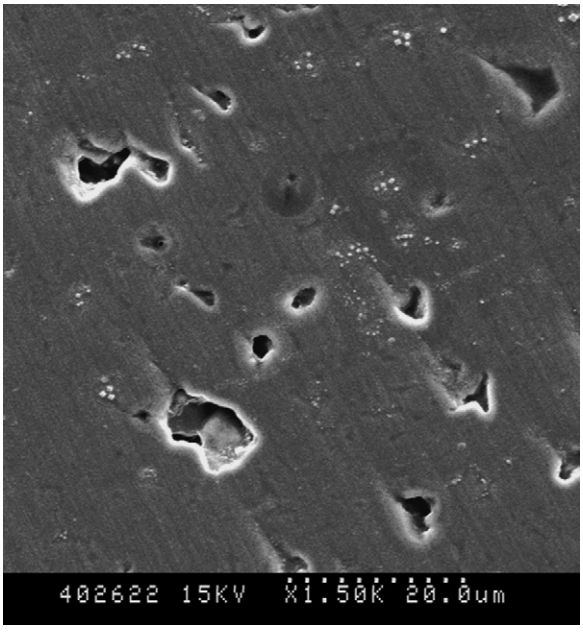

Fig. 9. SEM photomicrograph on polished surface of $AD_{10}F_0$ specimen.

pressureless sintering technology. Pores on polished surface of $AD_{10}F_0$ specimen (Fig. 9) are much fewer than that in AD_5F_0 and AD_5F_3 specimens (Figs. 7 and 8), which makes it clear that the addition of diopside decreases the amount of pores in large-scale fine structural alumina matrix ceramic guideway materials. Smaller gauge of pores are found in AD_5F_3 specimen (Fig. 8) by contrast to that in AD_5F_0 specimen (Fig. 7), indicating that the addition of Fe_2O_3 disperses pores in the guideway composites, incorporating into the same content of diopside.

4. Conclusion

Large-scale fine structural alumina matrix ceramic guideway materials were fabricated by pressureless sintering technology according to a temperature gradient. Liquid phase sintering takes place during the sintering process, during which new phases such as mullite, anorthite and $CaO{\cdot}6Al_2O_3$ were produced by the chemical reactions taking place among alumina and diopside. Addition of diopside and Fe_2O_3 significantly improves the performances of pressureless sintered guideway composites. The bending strength, fracture toughness and the hardness of $AD_{10}F_3$ specimen are 349.3 MPa, 4.32 MPa $m^{1/2}$ and 14.4 GPa, respectively, which are enhanced by 209.1%, 32.1% and 157.1%, respectively, with respect to pure Al_2O_3 pressureless sintered under the same conditions.

The shapes of pure alumina grains, unevenly distributed, are irregular and abnormal growth appears. Composites with the addition of diopside and Fe_2O_3 sintered under the same conditions show more homogeneous and finer microstructures. When the amount of diopside is identical, addition of Fe_2O_3 makes the microstructures of guideway composites a little more homogeneous and finer. The fracture mode of pure Al_2O_3 is mainly intergranular failure. While that of composites with addition of diopside and Fe_2O_3 is the combination of transgranular failure and intergranular failure, which may bring on the increases in bending strength and fracture toughness. Addition of diopside decreases the amount of pores in large-scale fine structural alumina matrix ceramic guideway materials. A small amount of Fe_2O_3 addition makes the pores smaller and more evenly distributed in the guideway composites, which may also contribute to the improvements in mechanical properties of large-scale fine structural alumina matrix ceramic guideway materials.

Acknowledgements

The work described in this paper is supported by the Ministry of Education, PR China (no. 03101) and the Outstanding Young Scientist Rewards of Shandong Province (no. 03BS103).

References

[1] E. Medvedovski, Alumina–mullite ceramics for structural applications, Ceram. Int. 32 (4) (2006) 369–375.

[2] D.W. Lee, B.K. Kim, Nanostructured Cu–Al_2O_3 composite produced by thermochemical process for electrode application, Mater. Lett. 58 (3/4) (2004) 378–383.
[3] G.S. Huang, Y. Xie, X.L. Wu, et al., Formation mechanism of individual alumina nanotubes wrapping metal (Cu and Fe) nanowires, J. Cryst. Growth 289 (1) (2006) 295–298.
[4] M. Jung, H.-G. Kim, J.-K. Lee, et al., EDLC characteristics of CNTs grown on nanoporous alumina templates, Electrochim. Acta 50 (2/3) (2004) 857–862.
[5] V. Viswabaskaran, F.D. Gnanam, M. Balasubramanian, Mullite from clay-reactive alumina for insulating substrate application, Appl. Clay Sci. 25 (1/2) (2004) 29–35.
[6] A. Aguilera, V. Jayaraman, S. Sanagapalli, et al., Porous alumina templates and nanostructured CdS for thin film solar cell applications, Solar Energy Mater. Solar Cells 90 (6) (2006) 713–726.
[7] S. Alini, A. Bottino, G. Capannelli, et al., Preparation and characterisation of Rh/Al_2O_3 catalysts and their application in the adiponitrile partial hydrogenation and styrene hydroformylation, Appl. Catal. A: Gen. 292 (2005) 105–112.
[8] Y. Zhang, M. Koike, R. Yang, et al., Multi-functional alumina–silica bimodal pore catalyst and its application for Fischer–Tropsch synthesis, Appl. Catal. A: Gen. 292 (2005) 252–258.
[9] A. Garron, K. Lázár, F. Epron, Effect of the support on tin distribution in Pd–Sn/Al_2O_3 and Pd–Sn/SiO_2 catalysts for application in water denitration, Appl. Catal. B: Environ. 59 (1/2) (2005) 57–69.
[10] B. Kasprzyk-Hordern, U. Raczyk-Stanisławiak, J. Świetlik, et al., Catalytic ozonation of natural organic matter on alumina, Appl. Catal. B: Environ. 62 (3/4) (2006) 345–358.
[11] S.I. Cha, K.T. Kim, K.H. Lee, et al., Strengthening and toughening of carbon nanotube reinforced alumina nanocomposite fabricated by molecular level mixing process, Scripta Mater. 53 (7) (2005) 793–797.
[12] S.K.C. Pillai, B. Baron, M.J. Pomeroy, et al., Effect of oxide dopants on densification, microstructure and mechanical properties of alumina–silicon carbide nanocomposite ceramics prepared by pressureless sintering, J. Eur. Ceram. Soc. 24 (2004) 3317–3326.
[13] W. Nakao, M. Ono, S.-K. Lee, et al., Critical crack-healing condition for SiC whisker reinforced alumina under stress, J. Eur. Ceram. Soc. 25 (16) (2005) 3649–3655.
[14] P.C. Ostertag, Influence of fiber and grain bridging on crack profiles in SiC fiber-reinforced alumina-matrix composites, Mater. Sci. Eng. A 260 (1/2) (1999) 124–131.
[15] E. Laarz, M. Carlsson, B. Vivien, et al., Colloidal processing of Al_2O_3-based composites reinforced with TiN and TiC particulates, whiskers and nanoparticles, J. Eur. Ceram. Soc. 21 (8) (2001) 1027–1035.
[16] P. Alizadeh, B. Eftekhary Yekta, A. Gervei, Effect of Fe_2O_3 addition on the sinterability and machinability of glass-ceramics in the system MgO–CaO–SiO_2–P_2O_5, J. Eur. Ceram. Soc. 24 (2004) 3529–3533.
[17] M. Rezvani, B. Eftekhari-Yekta, M. Solati-Hashjin, et al., Effect of Cr_2O_3, Fe_2O_3 and TiO_2 nucleants on the crystallization behaviour of SiO_2–Al_2O_3–CaO–MgO (R_2O) glass-ceramics, Ceram. Int. 31 (2005) 75–80.
[18] X.H. Zhang, C.X. Liu, J.H. Zhang, Research on the sintering process and performance of large-scale alumina matrix ceramic products, Mater. Sci. Forum 471/472 (2004) 821–824.
[19] Z.H. Jin, J.Q. Gao, G.H. Qiao, Engineering Ceramics [M], Publishing House of Xian Jiao Tong University, Xian, 2000 (in Chinese).
[20] R.F. Cook, B.R. Lawn, A modified indentation toughness technique, J. Am. Ceram. Soc. 66 (11) (1983) 200–201.
[21] D.L. Ye, J.H. Hu, Handbook of The Thermodynamic Data of Inorganic Substances, Metallurgical Industry Press, Peking, China, 2002pp. 57–1061.
[22] H.W. Kim, Y.H. Koh, H.E. Kim, Densification and mechanical properties of B_4C with Al_2O_3 as a sintering aid, J. Am. Ceram. Soc. 83 (11) (2000) 2863–2865.